Simulation of the Au(111)-$(22\times\sqrt{3})$ surface reconstruction

Yun Wang,[1] Noel S. Hush,[2] and Jeffrey R. Reimers[1,*]
[1]*School of Chemistry, The University of Sydney, New South Wales 2006, Australia*
[2]*School of Molecular and Microbial Biosciences, The University of Sydney, New South Wales 2006, Australia*
(Received 13 February 2007; published 27 June 2007)

The $(22\times\sqrt{3})$ reconstruction of the Au(111) surface is modeled using *a priori* density-functional theory simulations involving use of Born-Oppenheimer molecular dynamics and simulated annealing procedures. The reconstruction is exothermic by 0.43 eV per surface cell. Domains with surface atoms locating above fcc, hcp, and bridge sites of the second layer are produced, in quantitative agreement with experimental observations. While the reconstruction occurs to reduce the surface stresses created by cleavage of the bulk metal by minimizing the surface gold-gold interatomic separations, excess contraction appears associated with the bridge domains, causing them to stand out and form ridges above the surface. However, the chemical activity of the surface is reduced as the local surface density increases, making the fcc domain the most active part while the hcp domain and bridge ridges are less active.

DOI: 10.1103/PhysRevB.75.233416 PACS number(s): 68.35.Bs, 68.18.Fg, 68.37.Ef, 82.65.+r

Traditionally, gold has been regarded as having relatively inert surfaces, but recently gold nanoparticles on an oxide surface have been shown to catalyze CO or propane oxidation.[1] Further, it has been found that a clean gold surface has chemical activity when precovered with atomic oxygen.[2] Thiols reacted with gold surfaces are prominent in molecular-electronics applications, and the basic properties of the Au(111) surface, in particular, are of particular current interest.[3–6]

In particular, the initial stages of Au(111) monolayer production involve the interaction of the adsorbate molecules with a *reconstructed surface*: scanning tunneling microscopy (STM) studies have demonstrated that the bare Au(111) surface shows a $(22\times\sqrt{3})R30°$ reconstruction in which 46 surface atoms (in two rows along the $\langle 1\bar{1}0\rangle$ direction of 23 atoms each) occupy 44 bulklike positions.[3,4,7,8] These studies indicate that the reconstruction pushes some of the Au atoms sideways along the $\langle 11\bar{2}\rangle$ direction away from the usual fcc sites occupied by the surface layer toward the higher-energy hcp sites. In doing so, some gold atoms are forced to occupy even higher-energy bridge sites, thus elevating off the surface. As a result, the surface displays apparent grain boundary ridges between fcc-like and hcp-like valleys. Many detailed aspects of this reconstruction process remain unclear, however.

Basic understanding of the reconstruction process is provided through application of one-dimensional[9,10] and two-dimensional[11] Frenkel-Kontorova (FK) model[12–15] for surface reconstruction and through molecular dynamics (MD) simulations using empirical force fields.[16,17] These studies indicate[9] that cleavage of the bulk metal produces surface stress as the equilibrium interatomic distance $d_{\text{Au-Au}}$ preferred for surface atoms is less than that for bulk atoms; while such stress is a common feature of metal surfaces, the propensity to reconstruct is determined by both its magnitude and the magnitude of the interactions with the second layer that try to force the surface layer into compliant registry. Often, the parameters used in these models are obtained by applying density-functional theory (DFT) to simulate the structures of the bulk metal and the unreconstructed surface,[9] but no first-principles calculation has been performed that directly models the reconstruction. While the previous calculations allow major qualitative features such as the nature of the reconstruction and its propensity for different metals to be understood, they fail to reproduce details of the process such as the relative widths of the fcc and hcp domains, issues that are significant for the description of the chemical properties of the reconstructed surface.

In this Brief Report, the reconstructed Au(111) $(22\times\sqrt{3})$ surface is investigated through first-principles DFT calculations involving both simulated annealing studies using Born-Oppenheimer molecular dynamics and geometry optimizations. Our calculations reproduce details of the experimental observations including the widths of the fcc and hcp domains, depict how the surface is stabilized, understand the surface stress, and indicate variations in chemical reactivity across the reconstruction. This detailed information will assist in the understanding and prediction of a variety of chemical and physical processes occurring on the reconstructed Au (111) surface.

We employ plane-wave-based periodic DFT to investigate the reconstructed Au(111) $(22\times\sqrt{3})$ surface properties using the VASP program.[18] For the electron-electron exchange and correlation interactions, the functional of Perdew and Wang (PW91),[19] a form of the general gradient approximation, is used throughout. Electron-ion interactions are described using the optimized relativistic Vanderbilt-type ultrasoft pseudopotentials.[20] The plane-wave cut-off energy of 200 eV is applied. The Monkhorst-Pack k-point meshes used are $(1\times2\times1)$ and $(1\times4\times1)$ for the MD calculations and the final energies and geometry optimizations, respectively. A three-layer slab is used to model the Au(111) surface, such slabs being separated by a seven-layer thick vacuum region forming a three-dimensional periodic structure. The bottom layer of the slab is fixed at bulklike structure (a=4.18 Å), and the top two layers are allowed to relax upon optimization. To verify the convergence of our calculations with respect to enhancement of the above parameters, we have calculated the surface reconstruction energy [which is defined in Eq. (1) later] using various enhanced cut-off energies,

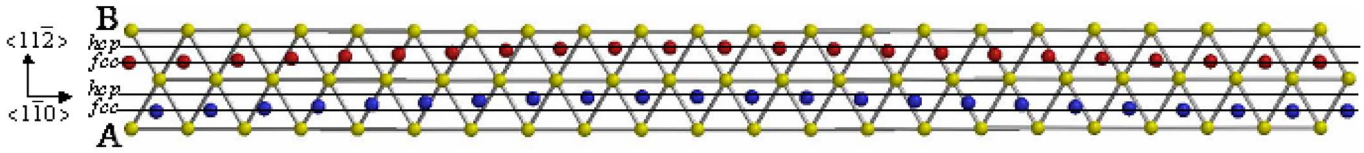

FIG. 1. (Color online) Top view of the reconstructed Au(111) $(22\times\sqrt{3})$ surface unit cell, highlighting the prevalent $\langle 1\bar{1}0\rangle$ and $\langle 11\bar{2}\rangle$ directions as well as the surface atoms in row A (blue) and row B (red) above the subsurface layer (yellow). The locations along the $\langle 11\bar{2}\rangle$ direction of the hcp and fcc sites above the subsurface layer are also indicated; the atoms in the surface layer are located near or between these high-symmetry locations.

k-point meshes, or layer thicknesses. The reconstruction energy changes by less than 0.01 eV when the cut-off energy increases to 270 eV or the number of layers is increased from 3 to 5; a larger but still not particularly significant change of 0.04 eV is found for a four-layer slab using a $(1\times6\times1)$ *k*-point mesh, however. In addition, we have compared the force on the surface atom obtained using three-layer and four-layer models. It is found that the force difference is quite small, less than 0.001 eV/Å. These results indicate that the parameters used in the simulations are adequate for our purposes.

To determine the structure of the reconstructed $(22\times\sqrt{3})$ surface, a two-step process is used. First, one additional Au atom is placed on the bridge site on the simpler unreconstructed (22×1) surface whose unit cell comprises a single row of 22 gold atoms. Then, MD is performed using the Nosé thermostat at temperatures of up to 573 K for 1.2 ps using a 4 fs time step. The system is then cooled to 0 K at a rate of 0.3 K fs^{-1}, and the annealed structure is then optimized at 0 K to achieve the stable configuration. Second, an initial model of the $(22\times\sqrt{3})$ reconstructed surface is obtained by taking this optimized row of atoms, called row A, and translating them to make a second row, row B. The simulated annealing procedure is repeated, heating at 573 K and then cooling to 0 K at a rate of 0.6 K fs^{-1} before final optimization. During this process, the translational symmetry of the two rows is lost, producing rather similar but distinctly different rows. This structure is shown in Fig. 1. At the ends of the depicted unit cell, the gold atoms on the top layer, colored blue and red in rows A and B, respectively, sit near fcc sites above the second layer. However, in the center of this cell, the atoms in the top layer are above hcp sites of the second layer. Horizontal black lines in the $\langle 1\bar{1}0\rangle$ direction on this figure indicate the $\langle 11\bar{2}\rangle$ coordinate of the fcc and hcp sites, and the locations of the top-layer atoms are seen to evolve gradually between the two extremum cases, passing through intermediary sites in which the atoms are above *bridge* positions of the second layer. The calculated maximum displacement of atoms in the $\langle 11\bar{2}\rangle$ direction is 0.77 Å, in excellent agreement with the experimental value of 0.7±0.3 Å.[7]

Detailed calculated structural properties of the reconstructed surface are shown in Fig. 2. The nearest-neighbor Au-Au distances $d_{\text{Au-Au}}$ in the topmost layer range between 2.80 and 2.87 Å and are all much shorter than the bulk gold-gold bond length optimized by the same method, 2.96 Å. The shortest distances are found for atoms above bridge sites of the second layer, while the fcc domain supports the largest separations. The hcp domain is noticeably different from the fcc one in that the maximum shortest separations are 0.02 Å less at 2.85 Å. Also, the contraction of the surface-layer bond lengths is associated with an increase in the separation

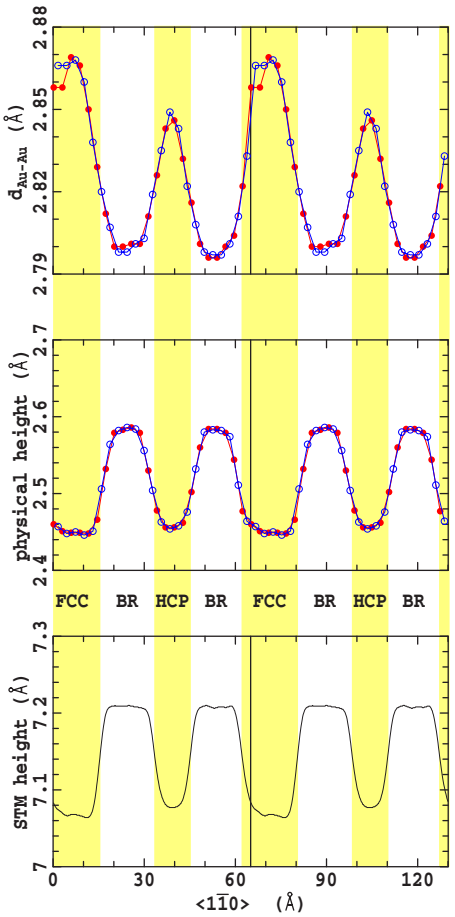

FIG. 2. (Color online) The structure of the topmost surface atoms in the reconstructed Au(111) $(22\times\sqrt{3})$ surface: (a) the shortest nearest-neighbor Au-Au distance $d_{\text{Au-Au}}$, (b) the height with respect to the average location of the second-layer atoms, and (c) the STM tip height obtained using the Tersoff-Hamann approximation at an electron density of 0.000 01 $e/Å^3$, averaged over the $\langle 11\bar{2}\rangle$ surface coordinate. The blue and red lines and dots correspond to atoms in rows A and B in Fig. 1, respectively, while the vertical shadings depict the fcc, hcp, and bridge ridge surface domains. Results are shown for two copies of the $(22\times\sqrt{3})$ lattice.

TABLE I. Percentage of various regions in the reconstructed Au (111) $(22\times\sqrt{3})$ surface. The experimental data are estimated based on STM images (Refs. 3 and 4).

	fcc	Ridge	hcp	Ridge
Experiment	34	22	22	22
Physical height	31	25	19	25
STM height	30	26	18	26

to the second layer. The interlayer distance is 2.41 Å for the unreconstructed surface, increasing after reconstruction to 2.46 Å for the fcc and hcp domains and 2.58 Å at the bridge ridges. The increase in height of 0.12 Å between the fcc and bridge locations is *double* that found for the binding of an adatom above fcc and bridge sites on a flat surface, indicating that the surface is locally expanded in these regions perhaps to avoid overly short nearest-neighbor Au-Au separations. The stress energy associated with this process can be roughly estimated by calculating the atomic gold adsorption energy difference of the structure at the fcc site, which is the most stable one on the regular Au(111) (2×2) surface, with that at the bridge site using the Au-surface height according to the reconstruction structure. The estimated stress energy at the ridges is 0.14 eV. As a reference, the corresponding energy at the fcc domain is very small, less than 0.01 eV; this indicates that the gold atoms in the fcc (and hcp) domains are in a more stable environment than are those located on the bridge ridges.

Figure 2 reveals that the calculations predict that the fcc domain is much wider than the hcp domain. Numerical estimates of the widths are obtained by dividing the surface into regions based on whether the height is less than the midpoint height of 2.52 Å (fcc and bridge domains) or greater than this value (bridge ridges), and the results are compared to experimental estimates in Table I. The experimental ratio of region sizes is approximately 1.5:1:1:1 or, as percentages, 34:22:22:22 for the fcc, first bridge ridge, hcp, and second bridge ridge, respectively, values which compare well to the calculated results of 31:25:19:25. As the Frenkel-Kontorova model calculations using the best available parameters predict equally sized fcc and hcp domains,[11] significant enhancements to the predicted structures are found through use of full *a priori* simulation techniques. In order to determine the cause of the differentiation in domain size, we evaluated the adsorption energy of a Au atom at the fcc site on the unreconstructed surface and found it to be lower than that at the hcp site by 0.02 eV. Such an energetic effect in itself would appear to be insufficient to explain the large structural differences, however. A more relevant property may be the surface stresses that drive the reconstruction. Clearly, the surface reconstructs in order to reduce surface bond lengths, but enhanced buckling found for the bridge domains [Fig. 2(b)] indicates that the reduction in the bridge ridges [Fig. 2(a)] is too great. As the reduction in the hcp regions is also greater than that in the fcc ones, a consequence of the presence of the close-lying third-layer atom, it may be modulations in the surface stress that induce the fcc-hcp asymmetry.

The experimental domain widths quoted above and in Table I are obtained from STM images, images that reflect not only the topological changes depicted in Fig. 2(b) but also changes in the electronic structure of the surface atoms. To model this additional effect, we simulate the STM image using the Tersoff-Hamann approximation[21] with an isocurrent model. Our simulated STM image is shown in Fig. 3. Most observed images are of lower resolution and depict only stripes, however, and to mimic this we averaged the image in the $\langle 11\bar{2}\rangle$ direction and smoothed it in the $\langle 1\bar{1}0\rangle$ direction using Gaussian broadening. The resulting averaged STM tip height is shown in Fig. 2(c) where it is seen to closely correspond to the topological height in Fig. 2(b). However, the feature changes have starker contrast, and the bridge ridges are more prevalent. Perceived feature widths extracted from this data are given in Table I. These are quite similar to the topology-only features and are close to, but slightly more removed from, the experimental results.

To understand the stability of the surface, the energy change for the reconstruction process is calculated using

$$\Delta E = E_{rec} - E_{un} - 2E_{\text{bulk}}, \tag{1}$$

where E_{rec} and E_{un} are the total energies with and without reconstruction, and E_{bulk} is the energy per Au atom of the bulk solid. Based on our calculations, the reconstruction energy is −0.43 eV per cell, demonstrating that the surface reconstruction process is significantly exothermic. According to the one-dimensional FK simulations, the lower total energy arises[9] from the difference between the surface stress released on reconstruction and the energy required to move the surface atoms away from the locations preferred by the interactions with the second layer. Another quantity of interest is the energy released on incorporation of gold atoms from top of an unreconstructed surface, evaluated to be 1.65 eV. The total energies between the reconstructed Au(111) $(22\times\sqrt{3})$ surface and the equivalent Au adatoms on the unreconstructed surface are also compared. Here, the adatoms adsorb at the fcc site, which is the most energetically preferential site. The total energy of the reconstructed surface decreases by 1.65 eV per cell. This indicates that the energy required to take a gold atom from the bulk to create an above-surface adatom is $(1.65-0.43)/2=0.61$ eV per adatom.

The electronic properties are analyzed by calculating the

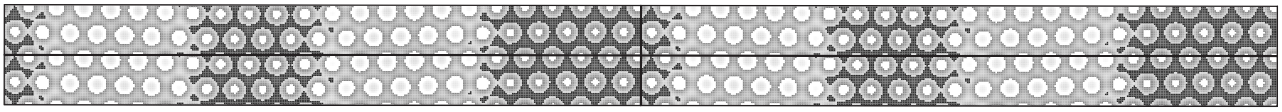

FIG. 3. Four copies of the simulated STM image of the reconstructed Au(111) $(22\times\sqrt{3})$ surface obtained using the Tersoff-Hamann approximation at an electron density of 0.000 01 $e/Å^3$.

Bader charge distribution.[22] It is found that the charge associated with each of the top-layer atoms is $\pm 0.05e$, and the total charge of the top layer is $0.02e$, where e is the magnitude of the charge on the electron. These charge polarizations are within the expected error (say, $0.1e$) associated with the determination of the gold surface from the finite grid of plane-wave basis set. Thus, there is no obvious charge transfer between the surface atoms induced by the reconstruction.

In order to understand the chemical activity of the reconstructed surface, atomic sulfur adsorption is used as the probe reaction. Sulfur has been selected due to the strong affinity between the sulfur atom and the Au(111) surface, and Au-S bonding is significant in self-assembled monolayer formation.[23] The adsorption properties of the sulfur atom on the unreconstructed Au(111) (2×2) surface are checked as a reference, and our results are similar to the former theoretical studies.[24] It is found that the fcc site is the most stable site among all the high-symmetry sites. Thus, we only study the case for sulfur at the fcc or fcc-like site on the reconstructed surface. Optimized structures were thus obtained with the sulfur atom absorbed at fcc-like sites in the center of the ridge, fcc, and hcp domains. The adsorption energy change is defined as

$$\Delta E = E_{tot} - E_{surf} - E_{ad}, \tag{2}$$

where E_{tot} and E_{surf} are the optimized total energies of the systems with and without adsorbate, respectively, and E_{ad} represents the energy of the isolated sulfur atom. It is found that the most energetically preferred area is the fcc domain. The adsorption energy on this domain is -3.67 eV, this structure being 0.23 and 0.27 eV more stable than adsorbates on the hcp and ridge domains, respectively. However, the adsorption on the fcc domain is 0.08 eV less exothermic than that at the fcc site on an unreconstructed (2×2) surface, indicating that the reconstruction reduces the surface activity slightly. The calculated surface activities parallel the shortest nearest-neighbor distances shown in Fig. 2(a): closely spaced atoms are less reactive. As only small surface charging effects are predicted to be associated with the reconstruction, these density fluctuations appear to control the chemical properties of the reconstructed surface.

In summary, we have reproduced the major qualitative and quantitative features of the Au(111) $(22\times\sqrt{3})$ surface reconstruction using *a priori* DFT simulations with the PW91 density functional. The reconstruction is predicted to be exothermic by 0.43 eV per surface cell. Domains with surface atoms locating above fcc, hcp, and bridge sites of the second layer are produced, in quantitative agreement with experimental observations. While the reconstruction occurs in order to reduce the surface stresses created by cleavage of the bulk metal by reducing the surface gold-gold interatomic separations, excess contraction appears associated with the bridge domains, causing them to stand out and form ridges above the surface. However, the chemical activity of the surface reduces as the local surface density increases, making the fcc domain the most active one and the bridge ridges the least active domain.

We thank the Australian Research Council for funding this work under the Discovery Grant program. The use of the supercomputer facilities at the Australia Partnership for Advanced Computing (APAC) is gratefully acknowledged.

*Author to whom correspondence should be addressed; FAX: +61 (2) 9351-3329; reimers@chem.usyd.edu.au

[1] M. Valden, X. Lai, and D. W. Goodman, Science **281**, 1647 (1998).
[2] J. L. Gong, R. A. Ojifinni, T. S. Kim, and M. K. Crommie, J. Am. Chem. Soc. **128**, 9012 (2006).
[3] W. Chen *et al.*, Phys. Rev. Lett. **80**, 1469 (1998).
[4] B. K. Min *et al.*, Top. Catal. **36**, 77 (2005).
[5] P. Pyykko, Angew. Chem., Int. Ed. **43**, 4412 (2004).
[6] J. D. Stiehl, T. S. Kim, S. M. McClure, and R. J. Behm, J. Am. Chem. Soc. **126**, 1606 (2004).
[7] J. V. Barth *et al.*, Phys. Rev. B **42**, 9307 (1990).
[8] J. Zhang, Q. Chi, and J. Ulstrup, Langmuir **22**, 6203 (2006).
[9] Z. Crljen, P. Lazic, D. Sokcevic, and R. Brako, Phys. Rev. B **68**, 195411 (2003).
[10] C. E. Bach, M. Giesen, H. Ibach, and T. L. Einstein, Phys. Rev. Lett. **78**, 4225 (1997).
[11] N. Takeuchi, C. T. Chan, and K. M. Ho, Phys. Rev. B **43**, 13899 (1991).
[12] J. Frenkel and T. Kontorova, Phys. Z. Sowjetunion **12**, 1 (1938).
[13] F. C. Frank and J. H. van der Merwe, Proc. R. Soc. London, Ser. A **198**, 205 (1949).
[14] A. Zangwill, *Physics at Surfaces* (Cambridge University Press, Cambridge, 1996).
[15] M. Mansfield and R. J. Needs, J. Phys.: Condens. Matter **2**, 2361 (1990).
[16] R. Ravelo and M. El-Batanouny, Phys. Rev. B **40**, 9574 (1989).
[17] S. Narasimhan and D. Vanderbilt, Phys. Rev. Lett. **69**, 1564 (1992).
[18] G. Kresse and J. Furthmüler, Comput. Mater. Sci. **6**, 15 (1996).
[19] J. P. Perdew and Y. Wang, Phys. Rev. B **45**, 13244 (1992).
[20] D. Vanderbilt, Phys. Rev. B **41**, 7892 (1990).
[21] J. Tersoff and D. R. Hamann, Phys. Rev. B **31**, 805 (1985).
[22] G. Henkelman, A. Arnaldsson, and H. Jonsson, Comput. Mater. Sci. **36**, 354 (2006).
[23] J. C. Love *et al.*, Chem. Rev. (Washington, D.C.) **105**, 1103 (2005).
[24] J. Gottschalck and B. Hammer, J. Chem. Phys. **116**, 784 (2002).